The Path Integral Monte Carlo Method

Riccardo Fantoni*

Università di Trieste, Dipartimento di Fisica, strada Costiera 11, 34151 Grignano (Trieste), Italy
(Dated: December 10, 2025)

We briefly review the Path Integral Monte Carlo method for an *exact* computer simulation of a quantum fluid in thermal equilibrium at a finite and non zero temperature.

Keywords: Computer Experiment; Path Integral; Monte Carlo

CONTENTS

* riccardo.fantoni@scuola.istruzione.it

I. INTRODUCTION

The basis for most *quantum simulations* is *imaginary time path integrals* [1].

Quite generally we will consider a fluid of particles of mass m in an Euclidean space at $R = (\{\boldsymbol{r}_i\}) = (\boldsymbol{r}_1, \boldsymbol{r}_2, \ldots)$ interacting with the following Hamiltonian

$$H = -\lambda \boldsymbol{\nabla}_R^2 + V(R), \tag{1.1}$$

where we denote with $\lambda = \hbar^2/2m$ and $\boldsymbol{\nabla}_R = \sum_i \boldsymbol{\nabla}_{\boldsymbol{r}_i}$ and V is the potential energy.

The *density matrix* of the fluid in thermal equilibrium at an inverse temperature $\beta = 1/k_B T$ with k_B the Boltzmann constant is

$$\rho(\beta) = e^{-\beta H}, \tag{1.2}$$

and satisfies to the *Bloch equation*

$$\frac{\partial \rho(\beta)}{\partial \beta} = -H \rho(\beta), \tag{1.3}$$

with the boundary condition

$$\rho(0) = \mathrm{Id} \tag{1.4}$$

where Id is the identity operator.

II. ALGORITHM DESCRIPTION

In a Path Integral Monte Carlo (PIMC) simulation of a fluid of N particles [1] at $R = (\boldsymbol{r}_1, \boldsymbol{r}_2, \ldots, \boldsymbol{r}_N)$ in d dimensions $\boldsymbol{r}_i = (r_{i,1}, r_{i,2}, \ldots, r_{i,d})$ in a region of space of measure Ω in thermal equilibrium at an inverse temperature β, we measure quantities $\mathscr{O}$, diagonal in position representation, through the following averaging

$$\langle \mathscr{O} \rangle = \frac{1}{Z} \sum_{\mathscr{P}} \mathrm{sgn}(\mathscr{P}) \int \rho(R, \mathscr{P}R; \beta) \mathscr{O}(R) \, dR, \tag{2.1}$$

where the sum is over all $N!$ permutations of the particles at R weighted with a sign $\mathrm{sgn}(\mathscr{P})$, the integral over R is multidimensional of dimension Nd, and [2]

$$\rho(R, R'; \beta) = \langle R | \rho(\beta) | R' \rangle = \int \prod_{k=0}^{M-1} [\rho(R_k, R_{k+1}; \tau) \, dR_k] \, \delta(R_0 - R) \delta(R_M - R') \, dR_M, \tag{2.2}$$

is the position representation of the density matrix where we have discretized the imaginary time β into M *timeslices* with a small *timestep* $\tau = \beta/M$, a *bead* $R_k = (\{\boldsymbol{r}_{i,k}\}) = (\{r_{i,j,k}\})$ at each timeslice $k = 1, 2, \ldots, M$, δ is a dN dimensional Dirac delta function. Here [3]

$$\rho(R, R'; \tau) = (4\pi\lambda\tau)^{-dN/2} e^{-(R-R')^2/4\lambda\tau} e^{-\tau V(R)}, \tag{2.3}$$

is the high temperature *primitive approximation* for the density matrix, and

$$Z = \sum_{\mathscr{P}} \mathrm{sgn}(\mathscr{P}) \int \rho(R, \mathscr{P}R; \beta) \, dR, \tag{2.4}$$

is the canonical *partition function*.

The high temperature density matrix of Eq. (2.3) holds for a fluid in a periodic hypercubic simulation box of side L in flat Euclidean space such that $L^2 \gg \lambda\tau$ [3]. In Appendix C we will present other expressions valid in the more general case of a Riemannian manifold

----

[1] We are excluding here anyonic statistics and internal properties of the particles like spin, ...

[2] This convolution product discretized path integral form is possible as long as *Trotter formula* [2] is valid which requires the potential energy to be bounded from below. This is not the case for a Coulomb system where it is necessary to construct the density matrix starting from a pair density matrix (see Appendix B) as building block.

[3] For a more general approximation form see Appendix A.

The integral in (2.2) is multidimensional of high dimension dNM. Then the rule for the measure in (2.1) can be recast into

$$\langle \mathcal{O} \rangle = \oint \Pi \mathcal{O} / \oint \Pi, \tag{2.5}$$

$$\Pi(\{R_k\}, \mathscr{P}) = \text{sgn}(\mathscr{P}) \prod_{k=0}^{M-1} \rho(R_k, R_{k+1}; \tau) \delta(R_0 - R) \delta(R_M - \mathscr{P}R) \tag{2.6}$$

$$= e^{-\mathscr{S}(s)} \text{sgn}(\mathscr{P}) \delta(R_0 - R) \delta(R_M - \mathscr{P}R), \tag{2.7}$$

$$\oint \ldots = \sum_{\mathscr{P}} \int dR_0 dR_1 \cdots dR_M \ldots, \tag{2.8}$$

where $\mathscr{S}(s) = \mathscr{K}(s) + \mathscr{V}(s)$ is the action and s is the $(\{R_k\})$ space. We require $\pi = \Pi / \oint \Pi$ to be a probability distribution. In other words it must be everywhere positive in the $(\{R_k\}, \mathscr{P})$ space. We will also need the splitting $\pi = \pi_0 \tilde{\pi}$ with $\tilde{\pi} = e^{-\mathscr{V}} / \oint \Pi$ the *inter-action distribution*. The action will then read

$$\mathscr{S}(s) = \sum_{k=0}^{M-1} \left\{ \frac{dN}{2} \ln(4\pi\lambda\tau) + \frac{(R_k - R_{k+1})^2}{4\lambda\tau} + \tau V(R_k) \right\}. \tag{2.9}$$

The *Monte Carlo method* (MC) [4] is a way to estimate numerically a highly multidimensional integral [4] and it is therefore ideally suited to evaluate a path integral like the one in Eq. (2.2).

Note that we have no knowledge on the partition function $Z = \oint \Pi$ since even a brute force Monte Carlo integration [4] will soon go into troubles due to the fact that the primitive approximation for the density matrix (2.3) is in general a function highly irregular in the $(\{R_k\}, \mathscr{P})$ space. We will then use the *Metropolis algorithm* [5] to sample π.

III. MONTE CARLO METHOD

A. Importance sampling

To calculate the expression in Eq. (2.5) [4] we introduce the probability distribution function P of importance sampling

$$\langle \mathcal{O} \rangle = \frac{\oint P[\Pi \mathcal{O}/P]}{\oint P[\Pi/P]}, \tag{3.1}$$

and we calculate

$$\langle \mathcal{O} \rangle = \frac{\sum_i \omega_i \mathcal{O}_i}{\sum_i \omega_i}, \tag{3.2}$$

where $\omega_i = \Pi_i/P_i$ and the sums are over C points distributed according to P. Then the variance of the measure

$$\sigma_{\mathcal{O}}^2 = \left\langle \left(\frac{\sum_i \omega_i \mathcal{O}_i}{\sum_i \omega_i} - \langle \mathcal{O} \rangle \right)^2 \right\rangle_P$$

$$= \frac{1}{\left(\sum_i \omega_i \right)^2} \left\langle \left[\sum_i \omega_i (\mathcal{O}_i - \langle \mathcal{O} \rangle) \right]^2 \right\rangle_P$$

$$\approx \frac{1}{\left(\sum_i \omega_i \right)^2} \left\langle \sum_i \omega_i^2 (\mathcal{O}_i - \langle \mathcal{O} \rangle)^2 \right\rangle_P$$

$$= \frac{1}{C \left(\int \Pi \right)^2} \left\langle \omega^2 (\mathcal{O} - \langle \mathcal{O} \rangle)^2 \right\rangle_P$$

$$= \frac{1}{C \left(\int \Pi \right)^2} \oint \frac{\Pi^2 (\mathcal{O} - \langle \mathcal{O} \rangle)^2}{P}, \tag{3.3}$$

---

[4] Which becomes more and more efficient than the usual quadrature methods as the number of dimensions increases. In general the MC integration becomes more efficient than a grid based integration as soon as the number of dimensions of the integral is bigger than twice the order of the quadrature integration scheme.

where we assumed that the sampled points were uncorrelated. Choosing $P = q^2/\oint q^2$ and solving the variational problem $\delta\sigma^2_{\mathscr{O}}/\delta q = 0$ one finds as optimal distribution

$$P^\star \propto |\Pi(\mathscr{O} - \langle\mathscr{O}\rangle)|. \tag{3.4}$$

Then usually one chooses

$$P = |\Pi|/\oint |\Pi|. \tag{3.5}$$

B. Sign problem

For bosons, $\mathrm{sgn}(\mathscr{P}) = 1$, we have no problems since Π is everywhere positive, but for fermions, $\mathrm{sgn}(\mathscr{P}) = (-1)^{\mathscr{P}}$, we find [6, 7]

$$\sigma^2_F = \sigma^2_B/\xi , \tag{3.6}$$

where the efficiency is

$$\xi = \left[\frac{\oint \Pi}{\oint |\Pi|}\right]^2 = \left[\frac{C_+ - C_-}{C}\right]^2 = \left[\frac{Z_F}{Z_B}\right]^2. \tag{3.7}$$

M_+/M is the average time the simulation spends in the positive region of Π and M_-/M the average time it spends in the negative region. The fermionic efficiency is proportional to the square of the average sign, Z_F is the partition function for fermions and Z_B the one for bosons. For example, from the results for the respective ideal (spinless) gases in the grand canonical ensemble

$$\xi = \begin{cases} e^{-N\rho^3\Lambda^3/(\sqrt{2})} & z \to 0 \\ e^{-N\rho 2(b_{5/2}(1) - f_{5/2}(1))/\Lambda^3} & z \to 1 \end{cases} \tag{3.8}$$

where $\Lambda = \sqrt{2\pi\beta\hbar^2/m}$ is the de Broglie thermal wavelength and $b_{5/2}(1) - f_{5/2}(1) \approx 0.4743$. We then see that for any fugacity z the efficiency becomes exponentially small in the number of particles. Moreover for fixed N we find in the canonical ensemble $\xi = e^{-2\beta(F_F - F_B)}$, with F the Helmholtz free energy, and in the high temperature limit [8]

$$\xi \approx e^{-2\rho N(2\pi\lambda\beta)^{3/2}}. \tag{3.9}$$

Whereas in the low temperature limit

$$F_F = F_F^0 - \frac{1}{4\lambda}\frac{N}{\beta^2}\left(\frac{\pi}{3\rho}\right)^{2/3}, \tag{3.10}$$

$$F_B = -\frac{N}{\beta}\frac{b_{5/2}(1)}{b_{3/2}(1)}\left(\frac{T}{T_c}\right)^{3/2}, \tag{3.11}$$

where $F_F^0 = N\epsilon_F + G_F^0$ with $\epsilon_F = \mu$ the Fermi energy, $G_F^0 = -\Omega\epsilon_F^{5/2}/(15\pi^2\lambda^{3/2})$, and $N = \Omega(2m\epsilon_F)^{3/2}/6\pi^2\hbar^3$. In the limit $\beta \to \infty$, we then find

$$\xi = e^{-2\beta F_F^0}, \tag{3.12}$$

with $F_F^0 = (1/6 - 1/15)\Omega\epsilon_F^{5/2}/(\pi^2\lambda^{3/2}) > 0$, which shows how the efficiency of a direct Monte Carlo calculation for fermions becomes exponentially small for increasing β and N, exactly where the physics becomes more interesting.

So even if the methods are exact, they become inefficient when one tries to use them on large systems or at low temperatures. But we do not know how to convert a fermion system into a path integral with a non negative integrand to avoid this "sign" problem.

All known general exact quantum simulation methods have an exponential complexity in the number of quantum degrees of freedom (assuming one is using a classical computer [9]). However, there are specific exceptions (solved problems) including thermodynamics of bosons, fermions in one dimension, the half-filled Hubbard model [10], and certain other lattice spin systems.

C. Random Walks

Let us start by reviewing the random walk or equivalently Markov chains. The application of these ideas have lead to one of the most important and pervasive numerical algorithm to be used on computers: the *Metropolis* algorithm first used by Metropolis, Rosenbluth and Teller in 1953 [5]. It is a general method of sampling arbitrary highly-dimensional probability distributions by taking a random walk through configuration space. Virtually all Quantum Monte Carlo simulations are done using either Markov sampling or a generalization of the Metropolis rejection algorithm. The Problem with simple sampling methods is that their efficiency goes to zero as the dimensionality of the space increases. Suppose we want to sample the probability distribution:

$$\pi(s) = \frac{\exp[-S(s)]}{Z}, \tag{3.13}$$

where $S(s)$ is the action. The partition function Z normalizes the function π in this space and is usually not known. A direct sampling method, requires sampling a function with a known normalization. Suppose we can directly sample a function $p_m(s)$. One can show that the Monte Carlo variance will depend on the ratio π/p_m. $\pi(s)$ is a sharply peaked function and it is very difficult to sample it directly because that would require knowing the normalization, or equivalently the exact partition function of a nearby related system, The efficiency would be related to the ratio of partition functions of the "model" systems to the real system which goes exponentially to zero as the number of dimensions increases.

Let us briefly review the properties of Markov chains. In a Markov chain, one changes the state of the system randomly according to a fixed *transition rule*, $\mathscr{P}(s \rightarrow s')$, thus generating a random walk through state space, $\{s_0, s_1, s_2 \ldots\}$. The definition of a Markov process is that the next step is chosen for a probability distribution fixed in "time" and depending only on the "present". This makes it very easy to describe mathematically. The process is often called the drunkard's walk. $\mathscr{P}(s \rightarrow s')$ is a probability distribution so that it satisfies

$$\sum_{s'} \mathscr{P}(s \rightarrow s') = 1, \tag{3.14}$$

and

$$\mathscr{P}(s \rightarrow s') \geq 0, \tag{3.15}$$

If the transition probability is *ergodic*, the distribution of s_n converges to a *unique equilibrium state*. That means there is a unique solution to:

$$\sum_{s} \pi(s)\mathscr{P}(s \rightarrow s') = \pi(s'). \tag{3.16}$$

The transition is ergodic if:

1. One can move from any state to any other state in a finite number of steps with a nonzero probability, i.e., there are no barriers that restrict any walk to a subset of the full configuration space.

2. It is not periodic. An example of a periodic rule is if the hopping on a bipartite lattice always proceeds from the A sites to the B sites so that one never forgets which site one started on. Non-periodic rule holds if $\mathscr{P}(s \rightarrow s) > 0$; if there is always some chance of staying put.

3. The average return time to any state is finite. This is always true in a finite system (e.g. periodic bomrdary conditions). It would be violated in a model of the expanding universe where the system gets further and further from equilibrium because there is no possibility of energy flowing between separated regions after the "big bang".

Under these conditions we can show that if $f_n(s)$ is the probability distribution of random walks after n steps, with $f_0(s)$ the initial condition, then:

$$f_n(s) = \pi + \sum_{\lambda} \epsilon_\lambda^n c_\lambda \phi_\lambda(s), \tag{3.17}$$

where the $\epsilon_\lambda < 1$. Hence the probability distribution converges exponentially fast to the stationary distribution π. Furthermore, the convergence is monotonic (it does not oscillate). Specifically, what we mean is that the distance between f_n and π is stricttly decreasing: $|f_n - \pi| > |f_{n+1} - \pi|$.

The transition probabilities often satisfy the *detailed balance* property for same function: the transition rate from s to s' equals the reverse rate,

$$\pi(s)\mathscr{P}(s \to s') = \pi(s')\mathscr{P}(s' \to s), \tag{3.18}$$

If the pair $\{\pi(s), \mathscr{P}(s \to s')\}$ satisfy detailed balance and if $\mathscr{P}(s \to s')$ is ergodic, then the random walk must eventually have π as its equilibrium distribution. To prove this fact, sum the previous equation over s and use Eq. (3.14) to simplify the right-hand-side. Detailed balance is one way of making sure that we sample π; it is a sufficient condition. Some methods work directly with the equilibrium Eq. (3.16) as we will see.

D. Metropolis algorithm

The Metropolis (rejection) method is a particular way of ensuring that the transition rule satisfy detailed balance. It does this by splitting the transition probability into an "a priori" *sampling distribution* $T(s \to s')$ (which is a probability distribution that we can sample) and an *acceptance probability* $A(s \to s')$ where $0 \leq A \leq 1$.

$$\mathscr{P}(s \to s') = T(s \to s')A(s \to s'), \tag{3.19}$$

In the generalized Metropolis procedure [4], trial moves are accepted according to:

$$A(s \to s') = \min[1, q(s' \to s)], \tag{3.20}$$

where

$$q(s \to s') = \frac{\pi(s')T(s' \to s)}{\pi(s)T(s \to s')}. \tag{3.21}$$

It is easy to verify detailed balance and hence asymptotic convergence with this procedure by looking at the 3 cases:

- $s = s'$ (trivial)

- $q(s \to s') \leq 1$

- $q(s \to s') \geq 1$

Two common errors are: first, if you can move from state s to s' then the reverse move must also be possible (both $T(s \to s')$ and $T(s' \to s)$ should be zero or non-zero together) and secondly moves that are not accepted are rejected and remain at the same location for at least one more step. Accepted or rejected steps contribute to averages in the same way.

Here is the generalized Metropolis algorithm:

1. Decide what distribution to sample($\pi(s)$) and how to move from one state to another, $T(s \to s')$

2. Initialize the state: pick s_0

3. To advance the state from s_n to s_{n+1}:

   - Sample s' from $T(s_n \to s')$
   - Calculate the ratio:

   $$q = \frac{\pi(s')T(s' \to s_n)}{\pi(s_n)T(s_n \to s')} \tag{3.22}$$

   - Accept or reject:
     If $q > 1$ or if $q > u_n$ where u_n is a uniformly distributed random number (RN) in (0,1) set $s_{n+1} = s'$.
     Otherwise set $s_{n+1} = s_n$.

4. Throw away the first κ states as being out of equilibrium

5. Collect averages every so often, and block them to get error bars

Consider the sampling of a probability distribution, $\exp[-S(s)]$. In the original Metropolis procedure, $T(s \to s')$ was chosen to be a constant distribution inside a segment (for a scalar field) and zero outside. This is the *classic* rule: a single field at a single lattice point is displaced uniformly, the segment length δ is adjusted to achieve 50% acceptance. Since T is a constant, it drops out of the acceptance formula. So the update rule is $s \to s'$ and accept or reject based on $\exp[-S(s') + S(s)]$. Moves that lower the action are always accepted. Moves that raise the action are often accepted if the action cost is small. Hence the random walk does not simply roll downhill. Fluctuations can drive it uphill.

Some things to note about Metropolis:

- One nice feature is that fields can be moved one at a time. And moves involving many fields at different lattice points may become inefficient.

- Note that we need both the forward probability and the reverse probability if one has a nonuniform transition probability. Also note that we cannot calculate the normalization of π-it is never needed. Only ratios enter in.

- The acceptance ratio (number of successful moves/total number of trials) is a key quantity to keep track of and to quote. Clearly if the acceptance ratio is very small, one is doing a lot of work without moving through phase space. On the other hand, if the acceptance ratio is close to 1, you could probably try larger steps and get faster convergence. There is a rule-of-thumb that it should be $1/2$, but in reality we have to look at the overall efficiency.

- One can show that the Metropolis acceptance formula is optimal among formulas of this kind which satisfy detailed balance.

- In some systems, it is necessary to have several different kinds of moves as in our case (see Section III E). So it is necessary to generalize the Metropolis procedure to the case in which one has a menu of possible moves. There are two ways of implementing such a menu. The simplest is to choose the type of move randomly, according to some fixed probability. One must include in the definition of $T(s \to s')$ the probability of selecting that move from the menu (unless you can argue that it cancels out.) A more common procedure is to go through all possible atoms systematically. After one pass, moves of all fields have been attempted once. In this case, individual moves do not satisfy detailed balance but it is easy to show that composition of moves is valid as long as each type of move individually satisfies detailed balance. Having many types of moves makes the algorithm much more robust, since before doing a calculation one does not necessarily know which moves will lead to rapid movement through phase space.

Since asymptotic convergence is easy to guarantee, the main issue is whether configuration space is explored thoroughly in a reasonable amount of computer time. Let us define a measure of the convergence rate and of the efficiency of a given Markov process. This is needed to compare the efficiency of different transition rules, to estimate how long the runs should be, and to calculate statistical errors. The rate of convergence is a function of the property being calculated. Generally one expects that there are local properties which converge quickly and other properties (such as order parameters near a phase boundary) which converge very slowly.

Let $\mathscr{O}(s)$ be a given property and let its value at step k of the random walk be $\mathscr{O}_k$. Let the mean and intrinsic variance of $\mathscr{O}$ be denoted by

$$\bar{\mathscr{O}} = \langle \mathscr{O} \rangle \tag{3.23}$$

and

$$\sigma_{\mathscr{O}}^2 = \langle (\mathscr{O}_k - \bar{\mathscr{O}})^2 \rangle \tag{3.24}$$

where the averages $\langle \dots \rangle$ are over π. These quantities depend only on the distribution π, not on the Monte Carlo procedure. We can show that the standard error of the estimate of the average, $\bar{\mathscr{O}}$, over a Markov chain with P steps, is

$$\text{error}[\bar{\mathscr{O}}] = \sqrt{\frac{\kappa_{\mathscr{O}} \sigma_{\mathscr{O}}^2}{P}}. \tag{3.25}$$

The *correlation time*, $\tau_{\mathscr{O}}$, defined as

$$\tau_{\mathscr{O}} = 1 + 2 \sum_{k=1}^{P} \frac{\langle (\mathscr{O}_0 - \bar{\mathscr{O}})(\mathscr{O}_k - \bar{\mathscr{O}}) \rangle}{\sigma_{\mathscr{O}}^2}, \tag{3.26}$$

gives the average number of steps to decorrelate the property $\mathcal{O}$. The correlation time will depend crucially on the transition rule and has a minimum value of 1 if one can move so far in configuration space that successive values are uncorrelated. In general, the number of independent steps which contribute to reducing the error bar from Eq. (3.25) is not P but P/τ.

Hence to determine the true statistical error in a random walk, one needs to estimate the correlation time. To do this it is very important that the total length of the random walk be much greater than $\tau_\mathcal{O}$. Otherwise the result and the error will be unreliable. Runs in which the number of steps is $P \gg \tau_\mathcal{O}$ are called *well converged*. In general, there is no mathematically rigorous procedure to determine τ. Usually one must determine it from the random walk. It is a good practice occasionally to run very long runs to test that the results are well converged.

The correlation time defined above is an equilibrium average. There is another correlation time relevant to Markov chains, namely, how many steps it takes to reach equilibrium from some starting state. Normally this will be at least as long as the equilibrium correlation time, but in some cases it can be much longer. The simplest way of testing convergence is to start the random walk from several, radically different, starting places and see if a variety of well-chosen properties converge to the same values. A starting place appropriate for a dense liquid or solid is with all the atoms sitting on lattice sites. However, it may take a very large number of steps for the initial solid to melt. Metastability and hysteresis are characteristic near a (first-order) phase boundary. A random starting place is with placing each variable randomly in the total space. It may be very difficult for the system to go to the equilibrium distribution from this starting place. More physical starting places are well-converged states at neighboring densities and temperatures.

The *efficiency* of a random walk procedure (for the property $\mathcal{O}$) is defined as how quickly the errors bars decrease as a function of computer time,

$$\xi_\mathcal{O} = \frac{1}{\tau_\mathcal{O} \sigma_\mathcal{O}^2 T}, \tag{3.27}$$

where T is the computer time per step. Hence the efficiency is independent of the length of the calculation and is the figure-of-merit for a given algorithm. The efficiency depends not only on the algorithm but also on the computer and the implementation. Methods that generate more steps per hour are, other things being equal, more efficient. We are fortunate to live in a time when the efficiency is increasing because of rapid advances in computers. Improvements in algorithms can also give rise to dramatic increases in efficiency. If we ignore how much computer time a move takes, an optimal transition rule is one which minimizes $\tau_\mathcal{O}$, since $\sigma_\mathcal{O}^2$ is independent of the sampling algorithm.

Usually transition rules are local; at a given step only a few fieldss are moved. If we try to move too many variables simultaneously, the move will almost certainly be rejected, leading to long correlation times. Given a transition rule, we deline the *neighborhood*, $\mathcal{N}(s)$, for each point in state space as the set of states s' that can be reached in a single move from s. (It is essential for detailed balance that the neighborhoods be reflexive. If s' is in the neighborhood of s, then s is in the neighborhood of s'.) With the *heat-bath* transition rule, one samples elements from the neighborhood with a transition probability proportional to their equilibrium distribution,

$$T_{HB}(s \to s') = \frac{\pi(s')}{C(s)}, \tag{3.28}$$

where the normalization constant is

$$C(s) = \sum_{s'' \in \mathcal{N}(s)} \pi(s''). \tag{3.29}$$

Then one sees, by substitution into the acceptance probability formula, that the acceptance probability will be

$$A(s \to s') = \min\left[1, \frac{C(s)}{C(s')}\right]. \tag{3.30}$$

If the neighborhood of s equals the neighborhood of s' then all moves will be accepted. For all transition rules with the same neighborhoods, the heat-bath rule will converge to the equilibrium distribution fastest and have the smallest correlation time. Within the neighborhood, with heat-bath one comes into equilibrium within a single step.

The heat-bath approach is not often used in continuum systems because the normalizations are difficult to compute; note that the integral in Eq. (3.29) extends over all space. For these systems the idea is to find a method close to the heat-bath rule, so that the correlation time is small, but with a transition rule which is able to be executed quickly.

E.   The moves

It is essential to use both a single bead, or single slice, move and a multiple bead move. The multiple bead move that we will describe is an efficient version of the more common Levy construction or Brownian bridge and is also crucial to sample permutations.

Single bead displacement

The simplest way to move a path is a uniform displacement of each of the dMN coordinate $\boldsymbol{r}_{i,k} \rightarrow \boldsymbol{r}_{i,k} + (1/2 - \eta)\boldsymbol{\Delta}$ for $i = 1, \ldots, N$ and $k = 1, \ldots, M$, where η is a uniform pseudo-random number in $[0, 1)$ and $\boldsymbol{\Delta}$ a fixed d-dimensional vector whose magnitude is chosen so to have acceptance ratios close to $1/2$. So that the transition probability density is just a constant and drops out of the acceptance probability.

The bisection method

The *bisection method* is a particular multilevel MC method [3, 11, 12]. Here we will use a slightly modified version employing correlated sampling. Choose a particle, say particle 1. The transition probability for the first level is chosen as $T_1 \propto \exp[(\boldsymbol{r}_{1,i+m/2} - \bar{\boldsymbol{r}})^2/2\sigma^2(m/2)]$ where $m = 2^l$, l being the number of levels, $\bar{\boldsymbol{r}} = (\boldsymbol{r}_{1,i} + \boldsymbol{r}_{1,i+m})/2$ and $\sigma(t_0/\tau) = \sqrt{\langle[\boldsymbol{r}_1(t) - (\boldsymbol{r}_1(t + t_0) + \boldsymbol{r}_1(t - t_0))/2]^2\rangle}$ (for the first levels these deviations are smaller than the free particle standard deviations used in the *Lévy construction* [13] $\sigma_f(\ell_k) = \sqrt{\ell_k \tau/2}$ with $\ell_k = m/2^k$ in the kth level). And so on for the other levels: $s_2 = \{\boldsymbol{r}_{1,i+m/4}, \boldsymbol{r}_{1,i+3m/4}\}$, ... , $s_l = \{\boldsymbol{r}_{1,i+1}, \boldsymbol{r}_{1,i+2}, \ldots, \boldsymbol{r}_{1,i+m-1}\}$. And $s_0 = \{\boldsymbol{r}_{1,0}, \ldots, \boldsymbol{r}_{1,i}, \boldsymbol{r}_{1,i+m}, \ldots, \boldsymbol{r}_{1,M-1}\}$ where i is chosen randomly. The *level inter-action distribution* is $\tilde{\pi}_k(s_0, \ldots, s_k) = \int ds_{k+1} \ldots ds_l \, \tilde{\pi}(s)$. For the kth level inter-action distribution we thus chose the following expression,

$$\tilde{\pi}_k \propto \exp\left[-\tau\ell_k \sum_{i=1}^{[M/\ell_k]} V(R_{i\ell_k})\right]. \tag{3.31}$$

In the last level $\ell_l = 1$ and the level inter-action distribution $\tilde{\pi}_l$ reduces to the exact inter-action distribution $\tilde{\pi}$. The acceptance probability for the first level will then be, $A_1 = \min\left[1, \frac{P_1(s)}{P_1(s')} \frac{\tilde{\pi}_1(s')\tilde{\pi}_0(s)}{\tilde{\pi}_1(s)\tilde{\pi}_0(s')}\right]$ with $P_1 \propto \exp\{-(\boldsymbol{r}_{1,i+m/2} - \bar{\boldsymbol{r}})^2[1/\sigma^2(m/2) - 1/\sigma_f^2(m/2)]/2\}$ and so on.

The permutations

Using the bisection method described above it is possible to realize the permutation of two particles chosen at random, say 1 and 2. It is enough to choose two beads distant m timeslices on particle 1, say $\boldsymbol{r}_{1,k}$ and $\boldsymbol{r}_{1,k+m}$ and the corresponding two beads on particle 2, $\boldsymbol{r}_{2,k}$ and $\boldsymbol{r}_{2,k+m}$. Then one proposes a move where with the bisection method a piece of path connecting $\boldsymbol{r}_{1,k}$ to $\boldsymbol{r}_{2,k+m}$ is constructed together with the other piece connecting $\boldsymbol{r}_{2,k}$ to $\boldsymbol{r}_{1,k+m}$ and the old pieces on each of the two particles are deleted. This, if accepted, produces an exchange of particle $1 \leftrightarrow 2$. The width m of the bisection can also be chosen at random during the simulation. Any permutation can then be reached through subsequent exchanges of pairs of particles.

IV.   PHYSICALLY MEASURABLE QUANTITIES

Once the action is chosen and sampling is accomplished, we are ready to calculate expectation values. In this section we discuss some of the technical details of constructing estimators for various physical quantities. What we need to do is to express a given quantum expectation of the density matrix as an average over a path as in Eq. (2.1). Properties can often be computed in different ways. A specific formula used to calculate some physical quantity is called an *estimator*. Each estimator is characterized by its statistical error, efficiency (statistical error for a given length run), bias (nonlinear distortion), timestep error, and finite size error. In addition, some estimators are easier physically to interpret or easier to program. These various criteria for what constitutes a good estimator make the choice rather subtle. Generally one wants an estimator that minimizes the maximum of the various errors.

A. The superfluid fraction

It is easy to determine when quantum statistics will be important in a fluid. In the absence of interaction, the size of a path is its thermal wavelength, the standard deviation of the position representation of the ideal gas density matrix

$$\Lambda_\beta = \sqrt{2\beta\lambda}, \tag{4.1}$$

When the size of the path equals the interparticle spacing, roughly $\rho^{-1/d}$ it is at least possible for the paths to link up by exchanging end points. This relations $\Lambda_\beta = \rho^{-1/d}$ defines the *degeneracy temperature*

$$T_d = \frac{\rho^{2/d}\hbar^2}{mk_B}. \tag{4.2}$$

For temperatures higher than T_d, quantum statistics (either bosonic or fermionic) are not very important.

In a liquid state, T_d gives a surprisingly good estimate of the *superfluid transition temperature* T_c.

Superfluidity is experimentally characterized by the response of a system to movements of its boundaries. The rotating bucket experiment was first discussed by Landau [14] on the basis of his two-fluids hydrodynamic theory of superfluidity. He predicted that superfluid helium would show an abnormal relation between the energy it takes to spin a bucket and its moment of inertia. Suppose one measures the work needed to bring a container filled with helium to a steady rotation rate. A normal fluid in equilibrium will rotate rigidly with the walls. The work done is $E = I\omega^2/2$, where I is the momentum of inertia and ω is the angular rotation rate. On the other hand, a superfluid will stay at rest if the walls rotate slowly, so that a smaller energy is needed to spin up the container. The liquid that stays at rest is the superfluid. Experiments by Andronikashvili [15] confirmed this prediction.

The microscopic properties of interacting Bose systems can be calculated by discretized pat integral computations of the density matrix [3, 16]. In these Monte Carlo simulations only the interparticle potential, $\hbar$, and the mass m of the particles are used. We consider a system of N particles in a volume Ω with a density $\rho = N/\Omega$ in thermal equilibrium at an inverse temperature $\beta = 1/k_B T$ with k_B Boltzmann constant.

We do not assume that the bucket has cylindrical symmetry, so there will be some coupling between the walls of the bucket and the liquid helium, allowing the liquid to come to thermal equilibrium with the walls. The effective moment of inertia is defined as the work done for an infinitesimally small rotation rate,

$$I = \left.\frac{dF}{d\omega^2}\right|_{\omega=0} = \left.\frac{d\langle \mathscr{L}_z\rangle}{d\omega}\right|_{\omega=0}, \tag{4.3}$$

where F is the Helmholtz free energy and $\mathscr{L}_z$ is the z component of the angular momentum

$$\mathscr{L} = -i\hbar\sum_{i=1}^{N}\boldsymbol{r}_i \times \boldsymbol{\nabla}_i, \tag{4.4}$$

where $\boldsymbol{\nabla}_i = \boldsymbol{\nabla}_{\boldsymbol{r}_i}$. On the other hand, the classical moment of inertia is given by

$$I_c = m\left\langle \sum_{i=1}^{N}(\boldsymbol{r}_i \times \hat{z})^2 \right\rangle. \tag{4.5}$$

The ration of the two moments is defined as the normal density ρ_n and what is missing is the superfluid density $\rho_s = \rho - \rho_n$

$$\frac{\rho_n}{\rho} = \frac{I}{I_c}. \tag{4.6}$$

Thus the superfluid density is the linear response to an imposed rotation, just as the electrical conductivity is the response to an imposed voltage.

We will here describe two Path Integral Monte Carlo (PIMC) estimators that can be used to measure the *superfluid fraction* $f_s = \rho_s/\rho \in [0,1]$ during a computer experiment [3].

Area estimator

Since statistical mechanics does not require the use of an inertial reference frame we can transform to the frame rotating with the bucket to determine the free energy of rotation. The Hamiltonian in the rotating coordinate system is simply given by

$$\mathscr{H}_\omega = \mathscr{H}_0 - \omega \mathscr{L}_z, \tag{4.7}$$

where $\mathscr{H}_0$ is the Hamiltonian at rest. Here the extra term comes from the relation $\theta' = \theta - \omega t$ between the new angle θ' in the rotating frame and the one θ in the laboratory frame.

Now we have to find a path integral expression for the effective moment of inertia defined in Eq. (4.3). The following identity allows us to take the derivative of the density matrix $e^{-\beta \mathscr{H}_\omega}$ that contains the parameter ω. First we break up the exponential into M pieces $e^{-\beta \mathscr{H}_\omega} = (e^{-\tau \mathscr{H}_\omega})^M$ with $\tau = \beta/M$,

$$\frac{de^{-\beta \mathscr{H}_\omega}}{d\omega} = \sum_{k=1}^{M} e^{-(k-1)\beta \mathscr{H}_\omega/M} \frac{de^{-\beta \mathscr{H}_\omega/M}}{d\omega} e^{-(M-k)\beta \mathscr{H}_\omega/M}. \tag{4.8}$$

Now we take the limit $M \to \infty$ and $k\beta/M \to t$

$$\frac{de^{-\beta \mathscr{H}_\omega}}{d\omega} = \int_0^\beta dt\, e^{-t\mathscr{H}_\omega} \frac{d(-\mathscr{H}_\omega)}{d\omega} e^{-(\beta-t)\mathscr{H}_\omega} = \int_0^\beta dt\, e^{-t\mathscr{H}_\omega} \mathscr{L}_z e^{-(\beta-t)\mathscr{H}_\omega}, \tag{4.9}$$

where in the last equality we used Eq. (4.7). So that Eq. (4.3) becomes

$$I = \mathrm{tr} \left(\int_0^\beta dt\, \mathscr{L}_z e^{-t\mathscr{H}_\omega} \mathscr{L}_z e^{-(\beta-t)\mathscr{H}_\omega} \right) / Z, \tag{4.10}$$

where $Z = \mathrm{tr}\left(e^{-\beta \mathscr{H}_\omega}\right)$ is the canonical partition function. Note that in general we should not assume that the system is invariant under rotations around the $\hat{z}$ axis so that we may not commute the angular momentum operator with the density matrix in the integrand of Eq. (4.10). Nonetheless we may use the cyclic property of the trace to reorder terms in the integrand.

Using Eq. (4.10) into Eq. (4.6) we express the normal fluid density ρ_n in terms of the matrix elements involving the system at rest. Now we explicitly evaluate this in terms of discrete path integrals by having the angular momentum operate on the action. Since angular momentum commutes with the internal potential energy, that term will not contribute. One can show [16] that an external potential also does not contribute in the continuum $M \to \infty$ limit. In evaluating the sum over k in Eq. (4.8) there is one tricky point. The $k = 1$ term must be treated separately, since $\mathscr{L}_z$ operates twice on one link. That term gives rise to the classical response. When $\mathscr{L}$ acts on the kth link of the high temperature density matrix $\rho_k \propto e^{-\sum_i (\boldsymbol{r}_{i,k} - \boldsymbol{r}_{i,k+1})^2/4\lambda\tau}$ we find $i\hbar \sum_i [\boldsymbol{r}_{i,k} \times (\boldsymbol{r}_{i,k} - \boldsymbol{r}_{i,k+1})]\rho_k/2\lambda\tau = -i\hbar(\boldsymbol{r}_{i,k} \times \boldsymbol{r}_{i,k+1})\rho_k/2\lambda\tau$, where the i index runs over the N particles, the k index labels the M timeslices and $\lambda = \hbar^2/2m$. Noticing that the two angular momentum operators acts on two independent links upon averaging over all the M links we arrive at the following result

$$f_s = \frac{\rho_s}{\rho} = 1 - \frac{\rho_n}{\rho} = \frac{2m\langle A_z^2 \rangle}{\beta\lambda I_c}, \tag{4.11}$$

$$\boldsymbol{A} = \frac{1}{2} \sum_{i,k} \boldsymbol{r}_{i,k} \times \boldsymbol{r}_{i,k+1}, \tag{4.12}$$

$$I_c = m \left\langle \sum_{i,k} (\boldsymbol{r}_{i,k} \times \hat{z}) \cdot (\boldsymbol{r}_{i,k+1} \times \hat{z}) \right\rangle. \tag{4.13}$$

Note that the area (4.12) of a path is a vector. For rotations about the z axis we need only the z component of the area. By symmetry the average value of $\boldsymbol{A}$ vanishes. Equation (4.11) is the main result of this section and is an exact fluctuation-dissipation formula. The superfluid density is proportional to the mean squared area of paths sampled for a container at rest divided by the classical moment of inertia.

Superfluidity is a microscopic property that can be defined in a finite system. It is not necessary to take the thermodynamic limit or to have a phase transition to see its effect. In the high temperature limit $f_s \to 0$ since the paths become short and straight and in the low temperature limit $f_s \to 1$ since the pat are long and the thermal average in Eq. (4.10) sums up to zero.

Winding estimator

Now let us change the geometry of the rotating cylinder, so we can see how superfluidity manifests itself in periodic boundary conditions. Periodic boundary conditions are more convenient for simulations, since no surfaces appear and there is no curvature in making a loop around the boundaries. Instead of using a filled cylinder, we enclose the fluid between two cylinders of mean radius R and spacing d, where $d \ll R$. The classical moment of inertia will be $I_c = mNR^2$ and the area (4.12) can be written as $A_z = WR/2$ where W is the *winding number*, defined as the flux of paths winding around the torus times the circumference of the torus. Here we have ignored all nonwinding paths, those paths which do not make a complete circuit around the cylinder, since their contribution is $\mathcal{O}(R^{-2})$ and negligible at large R. Now substituting these values of A_z and I_c, into Eq. (4.11) for the superfluid density and keeping into account the periodic boundary conditions along the d space dimensions (a hypertorus is topologically equivalent to the usual periodic boundary conditions), we get [5]

$$\frac{\rho_s}{\rho} = \frac{\langle W^2 \rangle L^2}{2d\lambda\beta N},$$
(4.14)

where the winding number is defined by

$$\boldsymbol{W} = \frac{1}{L} \sum_{i=1}^{N} \int_0^\beta dt \left[\frac{d\boldsymbol{r}_i(t)}{dt} \right].$$
(4.15)

Usually one applies periodic boundary conditions in all three spatial directions. Then the winding number becomes a vector, just as the area was a vector. But in contrast to the area, it is "quantized" in units of the box length. The winding number is a topological invariant of a given path; one can determine the winding number by counting the flux of paths across any plane; it does not matter where the plane is inserted. We can think of these winding paths as the imaginary time version of circulating currents.

In $d = 2$

It has been predicted theoretically [17, 18] and observed experimentally [19] that for [4]He films the superfluid density jumps from 0 to the universal value

$$\rho_s(T_c^-) = \frac{1}{\pi} \frac{k_B T_c^-}{\lambda}$$
(4.16)

just below the transition. In the present language this says that the average squared winding number, $\langle W^2 \rangle$, jumps from 0 to $4/\pi$ just below the transition, independent of particle density and periodic cell size.

B.   The momentum distribution

London [20] supposed the superfluid transition to be the analog of the transition that occurs in an ideal Bose gas where, below the transition, a finite fraction of particles occupy the zero-momentum state.

Penrose and Onsager [21] defined Bose condensation in an interacting system of atoms as the macroscopic occupation of a single-particle state, namely the state of zero momentum.

The *condensate fraction* has a simple meaning in terms of path integrals. Define the *single particle density matrix*

$$n(\boldsymbol{r}, \boldsymbol{r}') = \langle \delta(\boldsymbol{r}_1 - \boldsymbol{r}) \delta(\boldsymbol{r}_1' - \boldsymbol{r}') \rangle_n = \frac{\Omega}{Z} \int d\boldsymbol{r}_2 \ldots d\boldsymbol{r}_N \rho(\boldsymbol{r}, \boldsymbol{r}_2, \ldots, \boldsymbol{r}_N, \boldsymbol{r}'\boldsymbol{r}_2, \ldots, \boldsymbol{r}_N; \beta),$$
(4.17)

where here $\langle \ldots \rangle_n$ denotes an average over a probability distribution for paths open on the first particle with initial bead $\boldsymbol{r}_1$ and ending bead $\boldsymbol{r}_1'$, i.e. $(N-1)$ ring polymers and 1 open linear polymer. The single particle density matrix is normalized normalized as $\int d\boldsymbol{r}\, n(\boldsymbol{r}, \boldsymbol{r}) = \Omega$. The *momentum distribution*, the probability density of observing a single atom with momentum $\boldsymbol{k}$, is then

$$n_{\boldsymbol{k}} = \frac{1}{\Omega(2\pi)^d} \int d\boldsymbol{r} d\boldsymbol{r}'\, e^{-i\boldsymbol{k}\cdot(\boldsymbol{r}-\boldsymbol{r}')} n(\boldsymbol{r}, \boldsymbol{r}'),$$
(4.18)

———

[5] We could have made the whole derivation directly in the periodic space by calculating the response of a periodic system to a linear velocity of its walls. What appears in Eq. (4.10) in place of $\mathscr{L}$ is the total linear momentum operator [16].

normalized as $\int d\mathbf{k}\, n_{\mathbf{k}} = 1$. For an homogeneous and isotropic liquid we have $n(\mathbf{r}, \mathbf{r}') = n(|\mathbf{r} - \mathbf{r}'|)$ and $n(0) = 1$.

Then the condensate fraction, the probability of finding an atom with zero momentum, is

$$\tilde{n}_0 = \frac{(2\pi)^3}{\Omega} n_0 = \frac{1}{\Omega^2} \int d\mathbf{r} d\mathbf{r}'\, n(\mathbf{r}, \mathbf{r}'). \tag{4.19}$$

For a bulk isotropic and homogeneous liquid the single-particle density matrix in the superfluid state goes to a constant at large r (the momentum distribution, its Fourier transform, will then have a delta function at the origin), so

$$\tilde{n}_0 = \frac{1}{\Omega} \int d\mathbf{r}\, n(r), \tag{4.20}$$

and in the thermodynamic limit

$$\tilde{n}_0 = \lim_{r \to \infty} n(r). \tag{4.21}$$

The condensate fraction is essentially the probability of the two cut ends attaching themselves to a macroscopic exchange.

C. The energy

The internal energy is one of the main properties that one wants to get out of a simulation.

The direct estimator

We reach the *direct estimator* of the energy starting from

$$E_H = \langle H \rangle, \tag{4.22}$$

then acting with the Hamiltonian operator $H = -\lambda \nabla_R^2 + V$ on the kth link we find

$$\nabla_k \rho(R_k, R_{k+1}; \tau) = \left[-\frac{R_k - R_{k+1}}{2\lambda\tau} - \tau \nabla_k V(R_k) \right] \rho(R_k, R_{k+1}; \tau), \tag{4.23}$$

$$\nabla_k^2 \rho(R_k, R_{k+1}; \tau) = \left[\frac{R_k - R_{k+1}}{2\lambda\tau} + \tau \nabla_k V(R_k) \right]^2 \rho(R_k, R_{k+1}; \tau) +$$
$$\left[-\frac{dN}{2\lambda\tau} - \tau \nabla_k^2 V(R_k) \right] \rho(R_k, R_{k+1}; \tau), \tag{4.24}$$

where we denoted with $\nabla_k = \nabla_{R_k}$ the dN gradient respect to R_k. Therefore we find

$$E_H = \left\langle V(R_k) + \frac{dN}{2\tau} - \frac{(R_k - R_{k+1})^2}{4\lambda\tau^2} - \frac{(R_k - R_{k+1}) \cdot \nabla_k V(R_k)}{\tau} + \lambda\tau \nabla_k^2 V(R_k) - \lambda\tau^2 \left[\nabla_k V(R_k) \right]^2 \right\rangle. \tag{4.25}$$

The thermodynamic estimator

We reach the *direct estimator* of the energy starting from

$$E_T = -\frac{1}{Z} \frac{dZ}{d\beta} = -\frac{1}{ZM} \frac{dZ}{d\tau}, \tag{4.26}$$

then acting with the derivative on the kth link we find

$$E_T = \left\langle V(R_k) + \frac{dN}{2\tau} - \frac{(R_k - R_{k+1})^2}{4\lambda\tau^2} \right\rangle. \tag{4.27}$$

It is also possible to use the following thermodynamic estimator for the kinetic energy

$$K_T = \frac{m}{\beta} \frac{1}{Z} \frac{dZ}{dm} = -\frac{\lambda}{\beta} \frac{1}{Z} \frac{dZ}{d\lambda}, \tag{4.28}$$

then acting with the derivative on the kth link we find

$$K_T = \left\langle \frac{dN}{2\tau} - \frac{(R_k - R_{k+1})^2}{4\lambda\tau^2} \right\rangle. \tag{4.29}$$

$$V_T = \langle V(R_k) \rangle. \tag{4.30}$$

Recalling that $Z = e^{-\beta F}$ with F the Helmholtz free energy, from Eq. (4.26) we find $E_T = d(\beta F)/d\beta$ or

$$\beta_1 F_1 - \beta_0 F_0 = \int_{\beta_0}^{\beta_1} E_T \, d\beta. \tag{4.31}$$

The virial estimator

Consider the path integral expression (2.2) for the density matrix with C links

$$\rho(R_k, R_{k+C}; C\tau) = \int dR_{k+1} \cdots dR_{k+C-1} \, e^{-S}. \tag{4.32}$$

We must worry about periodic boundary conditions. The simplest way to do that is to change the integration variables from R_k to $\delta_k = R_k - R_{k-1}$. We shall always assume that τ is small enough that we can neglect paths that wrap around the boundary within a single step. Note that we are not neglecting paths that wind around the boundaries after c steps. The kinetic action depends only on δ_k. When R_k, is needed, in V or elsewhere, we shall define it in terms of the δ's

$$R_k = R_0 + \sum_{s=1}^{k} \delta_s. \tag{4.33}$$

Now we compute the energy as

$$E_{k,k+C} = -\frac{d \ln \rho(R_k, R_{k+C}; C\tau)}{d\tau} \tag{4.34}$$

Carrying out the derivative of the action (2.9) we find

$$E_{k,k+C} = \frac{dCN}{2\tau} + \sum_{s=1}^{C} \left\langle -\frac{\delta_{k+s}^2}{4\lambda\tau^2} + V(R_{k+s}) \right\rangle, \tag{4.35}$$

where $\langle \ldots \rangle$ indicates an average over $dR_{k+1} \cdots dR_{k+C-1}$.

Consider next the integral

$$G = \frac{1}{\rho(R_k, R_{k+C}; C\tau)} \sum_{s=1}^{C-1} \int d\delta_{k+1} \cdots d\delta_{k+C-1} (R_{k+s} - R_k) \cdot \nabla_{k+s} e^{-S}. \tag{4.36}$$

If we apply the ∇_{k+s} to the left, we see that $G = -dN(C-1)$. Since all surface terms will vanish for a sufficiently small τ. Applying the gradient to the right we find

$$G = -\left\langle \sum_{s=1}^{C-1} (R_{k+s} - R_k) \cdot \left[\frac{\delta_{k+s} - \delta_{k+s+1}}{2\lambda\tau} + \tau \nabla_{k+s} V(R_{k+s}) \right] \right\rangle. \tag{4.37}$$

This expression can be simplified with the identity

$$\sum_{s=1}^{C-1} (R_{k+s} - R_k) \cdot (\delta_{k+s} - \delta_{k+s+1}) = -\delta_{k+C} \cdot (R_{k+C} - R_k) + \sum_{s=1}^{C} \delta_{k+s}^2. \tag{4.38}$$

Using this identity inside Eq. (4.37) and eliminating the kinetic action with Eq. (4.35) we find

$$E_{k,k+C} = \left\langle \frac{dN}{2\tau} - \frac{\delta_{k+C} \cdot (R_{k+C} - R_k)}{4\lambda\tau^2} + \sum_{s=1}^{C} V(R_{k+s}) + \frac{1}{2} \sum_{s=1}^{C-1} (R_{k+s} - R_k) \cdot \nabla_{k+s} V(R_{k+s}) \right\rangle. \tag{4.39}$$

The internal energy is an average of E_C. One has to average over the end points as well as the intermediate R_k. We can also symmetrize both over the initial timeslice label and the direction of time. We have

$$E_V = \frac{1}{C}\langle E_{k,k+C}\rangle = \frac{1}{C}\langle E_{k,k-C}\rangle, \tag{4.40}$$

This gives the following *virial estimator*

$$E_V = \left\langle \frac{dN}{2C\tau} - \frac{1}{4C\lambda\tau^2}(R_{k+C} - R_k)\cdot(R_{k+1} - R_k) - \frac{1}{2}F_k\cdot\Delta_k + V(R_k)\right\rangle, \tag{4.41}$$

$$F_k = -\boldsymbol{\nabla}_k V(R_k), \tag{4.42}$$

$$\Delta_k = \frac{1}{2C}\sum_{s=-C+1}^{C-1}(R_k - R_{k+C}), \tag{4.43}$$

where F_k is the force.

The parameter C, with $1 \leq C \leq M$, is the window size for averaging. If it is chosen to be unity, then by inspection the virial estimator reduces to the thermodynamic estimator (4.26). Its maximum value is $C = M$ which is the conventional choice.

D.   The pressure

The thermodynamic pressure is defined as

$$P_T = -\left.\frac{dF}{d\Omega}\right|_\beta \tag{4.44}$$

$$= -\frac{1}{dL^{d-1}}\left.\frac{dF}{dL}\right|_\beta$$

$$= \frac{1}{dL^{d-1}\beta}\frac{1}{Z}\left.\frac{dZ}{dL}\right|_\beta$$

$$= \frac{1}{dL^{d-1}\beta}\left\langle\frac{dNM}{L} - \frac{\partial S}{\partial L}\right\rangle$$

$$= \frac{1}{d\Omega\tau}\left\langle dN - \frac{L}{M}\frac{\partial S}{\partial L}\right\rangle, \tag{4.45}$$

where in the second equality we used the $\Omega = L^d$, in the third $Z = e^{-\beta F}$, in the fourth we rescaled the coordinates as $X_k = R_k/L$ in the integral of Eq. (2.4) for the partition function, in the fifth we used $\beta = M\tau$.

Finally applying the derivative respect to L to the kth link in Eq. (2.9) for the action

$$P_T = \frac{1}{d\Omega\tau}\left\langle dN - \frac{(R_k - R_{k+1})^2}{2\lambda\tau} - \tau R_k\cdot\boldsymbol{\nabla}_k V(R_k)\right\rangle. \tag{4.46}$$

The virial theorem

From Eqs. (4.46) and (4.29) we find

$$P_T = \frac{1}{d\Omega}(2K_T + \langle W_k\rangle), \tag{4.47}$$

where $W_k = -R_k\cdot\boldsymbol{\nabla}_k V(R_k)$ is the *virial* on the kth link.

For example in a Coulomb liquid

$$W_k \propto \sum_{i<j=1}^{N}\frac{1}{|\boldsymbol{r}_{i,k} - \boldsymbol{r}_{j,k}|}, \tag{4.48}$$

so that from Eq. (4.30) follows $W_k = V(R_k)$ and

$$P_T = \frac{2K_T + V_T}{d\Omega}. \tag{4.49}$$

E. The isothermal compressibility

The isothermal compressibility is defined as follows

$$
\frac{1}{\chi_T} = -\Omega \left. \frac{dP}{d\Omega} \right|_\beta \tag{4.50}
$$

$$
= \Omega \left. \frac{d^2 F}{d\Omega^2} \right|_\beta
$$

$$
= \frac{1}{d^2 L^{d-2}} \left. \frac{d^2 F}{dL^2} \right|_\beta + \frac{d-1}{d} P
$$

$$
= -\frac{1}{d^2 L^{d-2} \beta} \frac{1}{Z} \left. \frac{d^2 Z}{dL^2} \right|_\beta + \beta \Omega P^2 + \frac{d-1}{d} P
$$

$$
= -\frac{1}{d^2 L^{d-2} \beta} \left\langle \frac{dNM(dNM-1)}{L^2} - \frac{2dNM}{L} \frac{\partial S}{\partial L} + \frac{\partial^2 S}{\partial L^2} \right\rangle + \beta \Omega P^2 + \frac{d-1}{d} P
$$

$$
= -\frac{1}{d\Omega\tau} \left\langle N(dNM-1) - 2NL \frac{\partial S}{\partial L} + \frac{L^2}{dM} \frac{\partial^2 S}{\partial L^2} \right\rangle + \beta \Omega P^2 + \frac{d-1}{d} P,
$$

$$
= -\frac{1}{d\Omega\tau} \left\langle \frac{L^2}{dM} \frac{\partial^2 S}{\partial L^2} \right\rangle + \frac{N(dNM+1)}{d\Omega\tau} - 2NMP + \beta \Omega P^2 + \frac{d-1}{d} P, \tag{4.51}
$$

where in the second equality we used the definition (4.44) of the pressure, in the third we used $\Omega = L^d$, in the fourth $Z = e^{-\beta F}$, in the fifth we rescaled the coordinates as $X_k = R_k/L$ in the integral of Eq. (2.4) for the partition function, in the sixth we used $\beta = M\tau$, and in the seventh we used Eq. (4.45).

Finally applying the derivative respect to L to the kth link in Eq. (2.9) for the action

$$
\frac{1}{\chi_T} = -\frac{1}{d^2 \Omega \tau} \left\langle \frac{(R_k - R_{k+1})^2}{2\lambda\tau} + \tau R_k \cdot \boldsymbol{\nabla}_k [R_k \cdot \boldsymbol{\nabla}_k V(R_k)] \right\rangle
$$

$$
+ \frac{N(dNM+1)}{d\Omega\tau} - 2NMP + \beta \Omega P^2 + \frac{d-1}{d} P, \tag{4.52}
$$

Appendix A: The residual energy

A more general form for an approximation to the high temperature density matrix is as follows

$$
\rho(R, R'; \tau) = \rho_0(R, R'; \tau) e^{-U(R, R'; \tau)}, \tag{A1}
$$

$$
\rho_0(R, R'; \tau) = (4\pi\lambda\tau)^{-dN/2} e^{-(R-R')^2/4\lambda\tau}. \tag{A2}
$$

The deviation from zero of the residual energy

$$
E_{\text{res}}(R, R'; \tau) = \frac{1}{\rho(R, R'; \tau)} \left(H + \frac{\partial}{\partial\tau} \right) \rho(R, R'; \tau) \tag{A3}
$$

is a measure of the quality of the primitive approximation chosen. Assuming all the particles of the same mass m, we find explicitly

$$
E_{\text{res}} = V(R) + \frac{1}{\rho} \left(-\lambda \boldsymbol{\nabla}_R^2 + \frac{\partial}{\partial\tau} \right) \rho(R, R'; \tau)
$$

$$
= V(R) + e^U \left(-\lambda \boldsymbol{\nabla}_R^2 + \frac{\partial}{\partial\tau} \right) e^{-U} + \frac{1}{\rho_0} \left(-\lambda \boldsymbol{\nabla}_R^2 + \frac{\partial}{\partial\tau} \right) \rho_0 - \frac{2\lambda}{\rho} \boldsymbol{\nabla}_R \rho_0 \cdot \boldsymbol{\nabla}_R e^{-U}
$$

$$
= V(R) - \frac{\partial U}{\partial\tau} - \frac{(R-R') \cdot \boldsymbol{\nabla}_R U}{\tau} + \lambda \boldsymbol{\nabla}_R^2 U - \lambda (\boldsymbol{\nabla}_R U)^2, \tag{A4}
$$

where $\lambda = \hbar^2 / 2m$.

So for the simpler form of the primitive approximation chosen in Eq. (2.3), where $U(R, R'; \tau) = \tau V(R)$ we find

$$
E_{\text{res}} = -(R - R') \cdot \boldsymbol{\nabla}_R V + \lambda\tau \boldsymbol{\nabla}_R^2 V - \lambda\tau^2 (\boldsymbol{\nabla}_R V)^2. \tag{A5}
$$

In table III of Ref. [3] we find an estimate of the residual energy for various kinds of approximations for the high temperature density matrix.

Appendix B: The pair density matrix

Consider a pair of particles in $d = 3$, one of mass m_1 at $\boldsymbol{r}_1$ and one of mass m_2 at $\boldsymbol{r}_2$ interacting with a pair potential $V(\boldsymbol{r})$ with $\boldsymbol{r} = \boldsymbol{r}_2 - \boldsymbol{r}_1$ their relative position vector. Their Hamiltonian will be

$$H = -\frac{\hbar^2}{2m_1}\boldsymbol{\nabla}^2_{\boldsymbol{r}_1} - \frac{\hbar^2}{2m_2}\boldsymbol{\nabla}^2_{\boldsymbol{r}_2} + V(\boldsymbol{r}), \tag{B1}$$

Introduce the center of mass coordinate $\boldsymbol{R} = (m_1\boldsymbol{r}_1 + m_2\boldsymbol{r}_2)/(m_1 + m_2)$ as shown in Fig. 1. We will also have

$$\begin{cases} \boldsymbol{r}_1 = \boldsymbol{R} - \frac{m_2}{M}\boldsymbol{r}, \\ \boldsymbol{r}_2 = \boldsymbol{R} + \frac{m_1}{M}\boldsymbol{r} \end{cases} \tag{B2}$$

where $M = m_1 + m_2$. It is a simple exercise to show that the Hamiltonian in relative coordinates $\boldsymbol{r}, \boldsymbol{R}$ becomes
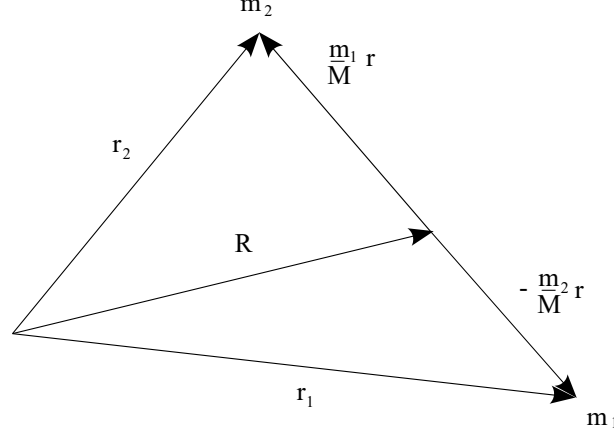

FIG. 1. Relative coordinates $\boldsymbol{r}, \boldsymbol{R}$.

$$H = -\frac{\hbar^2}{2M}\boldsymbol{\nabla}^2_{\boldsymbol{R}} - \frac{\hbar^2}{2\mu}\boldsymbol{\nabla}^2_{\boldsymbol{r}} + V(\boldsymbol{r}) = H_{\text{cm}} + H_{\text{rel}}, \tag{B3}$$

where $\mu = (1/m_1 + 1/m_2)^{-1}$ is the reduced mass and

$$\begin{cases} H_{\text{cm}} = -\lambda_{\text{cm}}\boldsymbol{\nabla}^2_{\boldsymbol{R}}, \\ H_{\text{rel}} = -\lambda_{\text{rel}}\boldsymbol{\nabla}^2_{\boldsymbol{r}} + V(\boldsymbol{r}). \end{cases} \tag{B4}$$

where $\lambda_{\text{cm}} = \hbar^2/2M$ and $\lambda_{\text{rel}} = \hbar^2/2\mu$.

The *pair density matrix* splits into

$$\rho = e^{-\beta H} = e^{-\beta H_{\text{cm}}}e^{-\beta H_{\text{rel}}} = \rho_{\text{cm}}\rho_{\text{rel}}. \tag{B5}$$

So the *center of mass density matrix* ρ_{cm} in coordinate representation is

$$\rho_{\text{cm}}(\boldsymbol{R}, \boldsymbol{R}'; \beta) = (4\pi\lambda_{\text{cm}}\beta)^{-3/2}e^{-(\boldsymbol{R}-\boldsymbol{R}')^2/4\lambda_{\text{cm}}\beta}. \tag{B6}$$

And the *relative density matrix* ρ_{rel} satisfies the Bloch equation

$$\frac{\partial \rho_{\text{rel}}}{\partial \beta} = -H_{\text{rel}}\rho_{\text{rel}}, \tag{B7}$$

with [22]

$$H_{\text{rel}} = -\lambda_{\text{rel}}\frac{1}{r^2}\frac{\partial}{\partial r}\left(r^2\frac{\partial}{\partial r}\right) + \lambda_{\text{rel}}\frac{\mathscr{L}^2}{r^2} + V(\boldsymbol{r}), \tag{B8}$$

where $\mathscr{L}$ is the angular momentum operator. Assuming spherical symmetry $V(\boldsymbol{r}) = V(r)$ the eigenfunctions of the relative Hamiltonian H_{rel} will be of the following form

$$\psi_{nlm}(\boldsymbol{r}) = R_n(r)Y_{lm}(\theta, \varphi), \tag{B9}$$

where Y_{lm} are the spherical harmonics. The relative density matrix will then have the following coordinate representation

$$\rho_{\text{rel}}(\boldsymbol{r}, \boldsymbol{r}'; \beta) = \sum_{n,l,m} e^{-\beta E_n} \psi_{nlm}^{\star}(\boldsymbol{r}) \psi_{nlm}(\boldsymbol{r}), \tag{B10}$$

where the sum is over the discrete and continuum spectrum. In Ref. [23] an efficient routine for calculating the pair Coulomb density matrix is given. In Refs. [24, 25] a theoretical improvement over the Pollock routine is proposed.

The cusp condition for the pair Coulomb density matrix

In a Coulomb system of point particles of charges $\{e_i\}$

$$V(R) = \sum_{i<j=1}^{N} e_i e_j v(r_{ij}) + C_N, \tag{B11}$$

$$v(r) = \begin{cases} 1/|\boldsymbol{r}| & d = 3 \\ -\ln(|\boldsymbol{r}|/\ell) & d = 2 \\ -|\boldsymbol{r}| & d = 1 \end{cases} \tag{B12}$$

where $\boldsymbol{r}_{ij} = \boldsymbol{r}_j - \boldsymbol{r}_i$, C_N is a constant needed to permit the existence of a thermodynamic limit in presence of the long range nature of the Coulomb potential [26], and ℓ is a constant of the dimensions of a length. The Coulomb pair potential is the solution of the Poisson equation in dimension $d = 1, 2, 3$

$$\delta v(\boldsymbol{r}) = -\varepsilon_d \delta^d(\boldsymbol{r}), \quad \varepsilon_d = \begin{cases} 4\pi & d = 3 \\ 2\pi & d = 2 \\ 2 & d = 1 \end{cases}, \tag{B13}$$

where δ^d is a d-dimensional Dirac delta function.

From the residual energy expression (A4) for $\tau = \beta$ we require $E_{\text{res}} = 0$. As two particles 1 and 2 approach each other, $r_{12} \to 0$, the other particles remaining a constant distance apart, we can expand $U(R, R'; \beta)$ in a power series in r_{12}. Using relative coordinates (B2) with $r = r_{12}$, assuming that the two particles approach each other in an isotropic, s, state, and equating terms diverging as $1/r_{12}$ one finds [23]

$$\lim_{r_{12} \to 0} \frac{\partial U(R, R'; \beta)}{\partial r_{12}} = -\frac{e_1 e_2}{(d-1)\lambda_{\text{rel}}}, \tag{B14}$$

where we used the following expression for the Laplacian in a Euclidean space of dimension d in an isotropic state

$$\boldsymbol{\nabla}_r^2 = \frac{\partial^2}{\partial r^2} + \frac{d-1}{r} \frac{\partial}{\partial r}. \tag{B15}$$

Appendix C: The high temperature density matrix on Riemannian manifolds

On a Riemannian manifold of dimension d and metric tensor $g_{\mu\nu}(\boldsymbol{r})$, the geodesic distance between two infinitesimally close points R and R' is $d\tilde{s}^2(R, R') = \sum_{i=1}^{N} ds^2(\boldsymbol{r}_i, \boldsymbol{r}_i')$ where $ds^2(\boldsymbol{r}, \boldsymbol{r}') = g_{\mu\nu}(\boldsymbol{r} - \boldsymbol{r}')^\mu (\boldsymbol{r} - \boldsymbol{r}')^\nu$. Moreover,

$$\tilde{g}_{\mu\nu}(R) = g_{\alpha_1 \beta_1}(\boldsymbol{r}_1) \otimes \ldots \otimes g_{\alpha_N \beta_N}(\boldsymbol{r}_N), \tag{C1}$$

$$\tilde{g}(R) = \prod_{i=1}^{N} \det ||g_{\alpha_i \beta_i}(\boldsymbol{r}_i)||, \tag{C2}$$

where $||\tilde{g}_{\mu\nu}||$ is a matrix made of N diagonal blocks $||g_{\alpha_i \beta_i}||$ with $i = 1, 2, \ldots, N$. The Laplace-Beltrami operator on the manifold of dimension dN is

$$\Delta_R = \tilde{g}^{-1/2} \boldsymbol{\nabla}_\mu (\tilde{g}^{1/2} \tilde{g}^{\mu\nu} \boldsymbol{\nabla}_\nu), \tag{C3}$$

where $\boldsymbol{\nabla} = \boldsymbol{\nabla}_R$, $\tilde{g}^{\gamma\nu}$ is the inverse of $\tilde{g}_{\gamma\nu}$, i.e. $\tilde{g}_{\mu\gamma} \tilde{g}^{\gamma\nu} = \delta_\mu{}^\nu$ the Kronecker delta, and a sum over repeated indexes is tacitly assumed.

We will assume that $\mathscr{H}$ in curved space has the same form (1.1) as in flat space [6]

$$\mathscr{H} = -\lambda \Delta_R + V(R). \tag{C4}$$

In the small τ limit Eq. (2.3) now becomes

$$\rho(R, R'; \tau) \propto \tilde{g}(R)^{-1/4} \sqrt{D(R, R'; \tau)}\, \tilde{g}(R')^{-1/4} e^{\lambda \tau \mathscr{R}(R)/6} e^{-\mathscr{S}(R, R'; \tau)}, \tag{C5}$$

where $\mathscr{R}$ is the scalar curvature of the curved manifold [7], $\mathscr{S}$ the action, and D the van Vleck's determinant [29, 30]

$$D_{\mu\nu} = \boldsymbol{\nabla}_\mu \boldsymbol{\nabla}'_\nu \mathscr{S}(R, R'; \tau), \tag{C6}$$

$$\det ||D_{\mu\nu}|| = D(R, R'; \tau), \tag{C7}$$

where $\boldsymbol{\nabla} = \boldsymbol{\nabla}_R$ and $\boldsymbol{\nabla}' = \boldsymbol{\nabla}_{R'}$. For this propagator the volume element for integration is $\sqrt{\tilde{g}(R)}\, dR$. In the expression (C5) the two factors $\tilde{g}^{-1/4}$ are needed in order to have for the density matrix a bidensity for which the boundary condition to Bloch equation is simply a Dirac delta function $\rho(R, R'; 0) = \delta(R - R')$. The square root of the van Vleck determinant factor takes into account the density of paths among the minimum extremal region for the action (see Chapter 12 of Ref. [30]).

For the *action* and the *kinetic-action* we have [8]

$$\mathscr{S}(R, R'; \tau) = \mathscr{K}(R, R'; \tau) + \tau V(R), \tag{C8}$$

$$\mathscr{K}(R, R'; \tau) = \frac{dN}{2} \ln(4\pi\lambda\tau) + \frac{d\tilde{s}^2(R, R')}{4\lambda\tau}. \tag{C9}$$

In particular the kinetic-action is responsible for a diffusion of the random walk with a variance of $2\lambda\tau/\tilde{g}_{\mu\nu}$.

On a sphere

A sphere of radius a is the surface, $d = 2$ [9], of constant positive scalar curvature $2/a^2$ so that $\mathscr{R} = 2N/a^2$ and in the small $\tau \to 0$ limit $\tilde{g}(R)^{-1/4} \sqrt{D(R, R'; \tau)}\, \tilde{g}(R')^{-1/4} \to (1/2\lambda\tau)^N$. So we see how both the curvature and the van Vleck factors, being constant, simply drop off from the measure of the various observables of Eq. (2.1). Yet from a calculation of one free quantum particle on the sphere we will face the *hairy ball theorem*, according to which the Euler class is the obstruction to the tangent plane of the sphere having a nowhere vanishing *section*, i.e. fiber or hair. The theorem was first proven by Henri Poincaré for the sphere in 1885 [31], and extended to higher even dimensions in 1912 by Luitzen Egbertus Jan Brouwer [32]. The theorem has been expressed colloquially as "you can't comb a hairy ball flat without creating a cowlick" or "you can't comb the hair on a coconut" as shown in Fig. 2. If z is a continuous function that assigns a vector in the three dimensional space to every point $\mathscr{P}$ on a sphere such that $z(\mathscr{P})$ is always tangent to the sphere at $\mathscr{P}$, then there is at least one pole, a point where the field vanishes, i.e. a $\mathscr{P}$ such that $z(\mathscr{P}) = 0$. Every zero of a vector field has a (non-zero) *index* [10], and it can be shown that the sum of all of the indexes at all of the zeros must be two, because the Euler characteristic of the sphere is two. Therefore, there must be at least one zero. This is a consequence of the *Poincaré-Hopf theorem*. The theorem was proven for two dimensions by Henri Poincaré and later generalized to higher dimensions by Heinz Hopf [33]. In particular we see how, even a single free particle have a path which will be subject to some anisotropy due to the effective potential induced by the curvature of the sphere. This effect was studied in Refs. [34, 35].

We plan in the near future to determine the superfluid fraction for a fluid of ^{4}He atoms on a sphere using the area estimator (4.11). We also plan to use affine quantization [27, 36] to fix the ordering ambiguities in Eq. (C4).

———

[6] This is a delicate point and should be studied more carefully [27]. Especially for what concerns ordering ambiguities. We here appeal to simplicity.

[7] The factor depending on the curvature of the manifold is due to Bryce DeWitt [28]. For a space of constant curvature there is clearly no effect, as the term due to the curvature just leads to a constant multiplicative factor that has no influence on the measure of the various observables. One might have hoped that certain constrained coordinates, perhaps a relative coordinate in a molecule, would effectively live in a space of variable curvature. Perhaps gravitation will give us the system on which the effect of curvature can be seen, but at present the effect is purely in the realm of theory.

[8] The expression for $\mathscr{K}$ is the one of Eq. (24.16) of Ref. [30] at lowest order.

[9] So it is conformally flat.

[10] The index of a bilinear function/al is the dimension of the space on which it is negative definite. According to Morse theorem, from the calculus of variations, there is a relation between the conjugate points (a point of the path where the path cease to be a minimum of the action) along a classical path to the negative eigenvalues of $\delta^2 S$. More precisely Morse index theorem states that, for an extremum $R(t), 0 < t < \beta$ of S, the index of $\delta^2 S$ is equal to the number of conjugate points to $R(0)$ along the path $R(t)$ (each such conjugate point is counted with its multiplicity). In the context of vector fields on a Riemannian manifold the index is equal to $+1$ around a source or a sink, and more generally equal to $(-1)^k$ around a saddle that has k contracting dimensions and $n - k$ expanding dimensions.
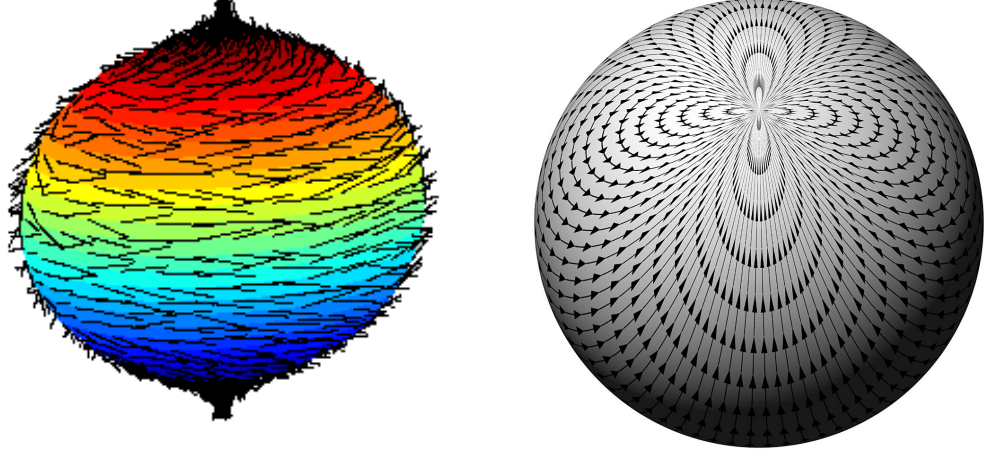
FIG. 2. On the left, pictorial view of a hairy ball; on the right, a continuous tangent vector field on a sphere with only one pole, in this case a dipole field with index 2. A path of a quantum particle on the sphere will be "combed".

AUTHOR DECLARATIONS

Conflicts of interest

None declared.

Data availability

The data that support the findings of this study are available from the corresponding author upon reasonable request.

Funding

None declared.

[1] R. P. Feynman, The λ-Transition in Liquid Helium, Phys. Rev. **90**, 116 (1953).
[2] H. F. Trotter, On the Product of Semi-Groups of Operators, Proc. Am. Math. Soc. **10**, 545 (1959).
[3] D. M. Ceperley, Path integrals in the theory of condensed Helium, Rev. Mod. Phys. **67**, 279 (1995).
[4] M. H. Kalos and P. A. Whitlock, *Monte Carlo Methods* (John Wiley & Sons Inc., New York, 1986).
[5] N. Metropolis, A. W. Rosenbluth, M. N. Rosenbluth, A. M. Teller, and E. Teller, Equation of state calculations by fast computing machines, J. Chem. Phys. **1087**, 21 (1953).
[6] D. M. Ceperley, Fermion Nodes, J. Stat. Phys. **63**, 1237 (1991).
[7] D. M. Ceperley, Path integral Monte Carlo methods for fermions, in *Monte Carlo and Molecular Dynamics of Condensed Matter Systems*, edited by K. Binder and G. Ciccotti (Editrice Compositori, Bologna, Italy, 1996) page 4.
[8] L. D. Landau and E. M. Lifshitz, *Statistical Physics*, Course of Theoretical Physics, Vol. 5 (Butterworth Heinemann, 1951) translated from the Russian by J. B. Sykes and M. J. Kearsley, edited by E. M. Lifshitz and L. P. Pitaevskii.
[9] R. P. Feynman, Simulating Physics with Computers, Int. J. Theor. Phys. **21**, 467 (1982).
[10] J. E. Hirsch, Two-dimensional Hubbard model: Numerical simulation study, Phys. Rev. B **31**, 4403 (1985).
[11] D. M. Ceperley and E. L. Pollock, Path-integral computation of the low-temperature properties of liquid ^{4}He, Phys. Rev. Lett. **56**, 351 (1986).
[12] D. M. Ceperley and E. L. Pollock, Path-integral simulation of the superfluid transition in two-dimensional ^{4}He, Phys. Rev. B **39**, 2084 (1989).

[13] P. Lévy, Sur certains processus stochastiques homogènes, Compositio Math. **7**, 283 (1939).

[14] L. D. Landau, The theory of superfuidity of helium II, J. Phys. USSR **5**, 71 (1941).

[15] E. L. Andronikashvili, A direct observation of two kinds of motion in helium II, J. Phys. USSR **10**, 201 (1946).

[16] E. L. Pollock and D. M. Ceperley, Path-integral computation of superfluid densities, Phys. Rev. B **36**, 8343 (1987).

[17] J. M. Kosterlitz and D. J. Thouless, Ordering, metastability and phase transitions in two-dimensional systems, J. Phys. C: Solid State Phys. **6**, 1181 (1973).

[18] D. R. Nelson and J. M. Kosterlitz, Universal Jump in the Superfluid Density of Two-Dimensional Superfluids, Phys. Rev. Lett. **39**, 1201 (1977).

[19] J. Bishop and J. D. Reppy, Study of the Superfluid Transition in Two-Dimensional ^{4}He Films, Phys. Rev. Lett. **40**, 1727 (1978).

[20] F. London, On the Bose-Einstein Condensation, Phys. Rev. **54**, 947 (1938).

[21] O. Penrose and L. Onsager, Bose-Einstein Condensation and Liquid Helium, Phys. Rev. **104**, 576 (1956).

[22] L. D. Landau and E. M. Lifshitz, *Quantum mechanics*, Course of Theoretical Physics, Vol. 3 (Butterworth Heinemann, 1977) translated from the Russian by J. B. Sykes and M. J. Kearsley, edited by E. M. Lifshitz and L. P. Pitaevskii. Section §32.

[23] E. L. Pollock, Properties and computation of the Coulomb pair density matrix, Comput. Phys. Commun. **52**, 49 (1988).

[24] P. Vieillefosse, Coulomb Pair Density Matrix I, J. Stat. Phys. **74**, 1195 (1994).

[25] P. Vieillefosse, Coulomb Pair Density Matrix II, J. Stat. Phys. **80**, 461 (1995).

[26] V. Natoli and D. M. Ceperley, An Optimized Method for Treating Long-Range Potentials, Comput. Phys. **117**, 171 (1995).

[27] J. R. Klauder and R. Fantoni, The Magnificent Realm of Affine Quantization: valid results for particles, fields, and gravity, Axioms **12**, 911 (2023).

[28] B. S. DeWitt, Dynamical Theory in Curved Spaces. I. A Review of the Classical and Quantum Action Principles, Rev. Mod. Phys. **29**, 377 (1957).

[29] J. H. V. Vleck, The Correspondence Principle in the Statistical Interpretation of Quantum Mechanics, Proc Natl Acad Sci U S A **14**, 178 (1928).

[30] L. S. Schulman, *Techniques and Applications of Path Integration* (John Wiley & Sons, Technion, Haifa, Israel, 1981) chapter 24.

[31] H. Poincaré, Sur les courbes dfínies par les quations diffréntielles, Journal de Mathématiques Pures et Appliqués **4**, 167 (1885).

[32] L. E. J. Brouwer, Über Abbildung von Mannigfaltigkeiten, Mathematische Annalen **71**, 97 (1912).

[33] H. Hopf, Vektorfelder in n-dimensionalen Mannigfaltigkeiten, Math. Ann. **96**, 209 (1926).

[34] R. Fantoni, One-component fermion plasma on a sphere at finite temperature, Int. J. Mod. Phys. C **29**, 1850064 (2018).

[35] R. Fantoni, One-component fermion plasma on a sphere at finite temperature. The anisotropy in the paths conformations, J. Stat. Mech. , 083103 (2023).

[36] R. Fantoni, *Unifying Classical and Quantum Physics - How classical and quantum physics can pass smoothly back and forth* (Springer, New York, 2025).